J. Fluid Mech. (1982), *vol.* 123, *pp.* 335–362
Printed in Great Britain

Comparison of conditional sampling and averaging techniques in a turbulent boundary layer

By C. S. SUBRAMANIAN, S. RAJAGOPALAN, R. A. ANTONIA AND A. J. CHAMBERS
Department of Mechanical Engineering, University of Newcastle, N.S.W. 2308, Australia

(Received 28 January 1981 and in revised form 26 January 1982)

Visual examination of simultaneous temperature traces from a rake of cold wires placed across a turbulent boundary layer had enabled the identification of coherent temperature fronts. An X-wire/cold-wire arrangement was used simultaneously with the rake to provide measurements of the velocity fluctuations u (longitudinal) and v (normal) and the temperature fluctuation θ. Conditional averages of u, v, θ and products uv, $u\theta$, $v\theta$ were obtained by application of conditional techniques based on the detection of the temperature fronts using information obtained at only one point in space. These averages, obtained at various positions across the layer, have been compared with those obtained when the rake was used to detect the fronts. The comparison has indicated that none of the one-point detection techniques is in good quantitative agreement with the rake detection technique, the largest correspondence between the rake technique and any of the other one-point techniques being only 51 %. With the exception of the hole technique used in conjunction with the quadrant decomposition analysis, conditional averages obtained from one-point techniques are in reasonable qualitative agreement with those deduced using the rake.

1. Introduction

A great deal of information on coherent structures in a turbulent boundary layer has been obtained from flow-visualization studies. The study of Kline *et al.* (1967) and the pipe-flow study of Corino & Brodkey (1969) established the presence and importance in the wall region of a sequence of events that is now referred to as the bursting phenomenon. This sequence consists of the formation of low-speed streaks aligned with the flow direction with subsequent lift up away from the wall of part of these streaks. In the ejection phase, the lifted streaks become unstable, oscillate and break down. This phase is then followed by a sweep phase where high-momentum fluid that originates in the outer layer moves towards the wall with a relatively shallow angle. More recently, Head & Bandyopadhyay (1978, 1981) have suggested, on the basis of observations of a smoke-filled boundary layer, that the layer consists almost exclusively of a fairly ordered array of vortex loops or hairpins, some of which extend through the complete thickness of the layer. The relation between these vortex loops and the observed events near the wall is not well understood. It is also not clear how the vortex loops or hairpins fit in with what has been described as the large-scale motion, especially when the Reynolds number is relatively large.

While flow-visualization studies have provided useful qualitative and, in a few instances, quantitative information about coherent structures in turbulent shear flows, most of the quantitative information has been obtained with the use of the conditional sampling and averaging technique. For the present purpose, conditional

sampling can be defined as the eduction of information about a coherent structure with respect to the time reference provided by the detection method used to recognize the structure. While conditional sampling has helped (see e.g. Kaplan 1973; Antonia 1980, 1981) to bridge the gap between data collected in Eulerian and Lagrangian reference frames there is inevitable arbitrariness associated with the selection of the detection criteria. Differences exist (these will be discussed later) between quantitative results obtained by different detection methods supposedly focusing on the same structure. The onus is therefore on the experimentalist to demonstrate that the structure recognized is not an artifact of the detection method used. Most, if not all, investigators who have used conditional sampling and averaging have ensured that their particular detection method does not educe a structure when it is applied to a pseudoturbulent structureless signal (see e.g. Blackwelder & Kaplan 1976, referenced hereinafter as BK; Wallace, Brodkey & Eckelmann 1977; Thomas 1977). This test, although important, is not sufficient, and there is clearly a need to establish the validity and accuracy of quantitative data yielded by conditional techniques before the question of how important a role in momentum, heat and mass transfer these structures play can be answered. A critical comparison of different detection methods would be helpful in establishing the accuracy of quantitative data.

Offen & Kline (1973, 1975) used hot-film anemometry and synchronized motion-picture records of dye visualization in the wall region of a boundary layer to compare several burst-detection schemes (using only velocity data) with the visual indications of bursting. Included in the detection schemes that were used were the VITA (variable-interval time-averaging) technique used by BK, and the HOLE technique used by Lu & Willmarth (1973). The combined anemometer/dye experiments indicated that none of the detection schemes correlated very well with the visual indications of bursting or with any other scheme. Offen & Kline suggested that serious doubts existed about which events were measured by each detection scheme. Nonetheless, most schemes detected at least some portion of 43 %–59 % of the visual ejections when the detection criteria of these schemes were adjusted to yield a total number of detections approximately equal (≈ 81) to the number of visually observed ejections. When the detection criteria's on–off time functions (equal to unity when the structure is detected and zero otherwise) were correlated, the maximum correlation coefficient associated with any pair of schemes was in the range 0·35–0·42. Despite this poor correlation, Offen & Kline emphasized that the schemes agreed with each other to a certain extent in their relationships to the visual data, and many of them were as effective as the visual data at detecting periods of large uv.

In the present study, a rake of cold wires is used in a slightly heated boundary layer to identify the spatially coherent rapid decrease in temperature described by Chen (1975) and Chen & Blackwelder (1978), referenced hereinafter as CB, as a sharp internal temperature front.† This three-dimensional front, of spanwise scale‡ of order of the boundary-layer thickness, was associated with the back of a turbulent bulge in the outer part of the layer. Conditional averages of u and v measured by CB suggested that an internal shear layer was associated with the temperature front and that this shear layer 'provided a dynamical relationship between the large structures

† CB's terminology is retained here – although it may be slightly confusing since the front has been identified with the back of a turbulent bulge. It should also be noted that Sunyach (1971) had identified coherent, sharp temperature gradients on temperature traces obtained with a rake of six temperature sensors in a two-dimensional mixing layer.

‡ Using information obtained from a spanwise rake of hot wires, Thomas (1977) concluded that the spanwise scale of the large structure is of the order of the boundary-layer thickness.

in the outer, intermittent region and the bursting phenomenon'. It was felt that the effectiveness of conditional techniques, based essentially on information derived at one point in space, could be usefully tested by comparing conditional averages obtained by these techniques with those obtained with the rake method, since the latter provides simultaneous information over a relatively extensive region of space. Two conditional techniques examined here are VITA and HOLE, the techniques used by Offen & Kline to detect ejections near the wall. As in the work of Offen & Kline, one motivation for the present investigation was that the comparison would, we hoped, suggest a conditional technique that would reliably detect the temperature front without having to resort to the relatively cumbersome rake method of detection.

2. Experimental arrangements and conditions

The boundary layer developed, with zero pressure gradient, over the smooth floor of the working section (0·38 m × 0·23 m) of the wind tunnel. The first 3 m of the working-section floor consists of 20 identical electrically heated Inconel strips (30 cm × 15 cm × 0·046 cm) supported by a Sindanyo (hard asbestos board) base plate. The strips are insulated from each other and connected in series to provide a uniform wall-heat-flux distribution. The last 1·83 m of the working-section floor are unheated and consist of epoxy-coated Sindanyo board. A 3 mm diameter wire was placed on the heated wall at 4 cm from the entrance of the working section to trip the boundary layer. This location of the trip was such that virtual origins of the momentum and thermal layers, as determined from the streamwise variation of momentum and enthalpy thickness, were approximately coincident. The matching of virtual origins was achieved using a procedure similar to that suggested by Perry & Hoffmann (1976), who avoided the effect of an unheated starting length by a trial-and-error process of shifting the boundary-layer trip.

Mean- and fluctuating-temperature measurements were made with a 0·6 μm Pt–10 % Rh cold wire (resistance thermometer) (temperature coefficient of $1{\cdot}5 \times 10^{-3}$ °C^{-1}) operated by a constant-current (0·1 mA) anemometer. Mean-velocity measurements were made with a 5 μm Pt–10 % Rh wire, operated by a DISA 55M10 constant-temperature anemometer at an overheat ratio of 1·8. A rake (see figure 1) of 11 cold wires (0·6 μm Pt–10 % Rh, length = $0{\cdot}8 \pm 0{\cdot}1$ mm) was constructed using double-sided printed-circuit board. Details of the construction are given in Subramanian (1981). Wires at locations 1 and 11 in figure 1 were at nominal values of y/δ equal to 0·007 and 0·93 respectively. Simultaneous measurements of u, v, θ were made with an X-wire and a cold wire located 1·2 mm upstream of the geometrical centre of the X-wire and in a direction perpendicular to the plane of the X-wire. The X-wire/cold-wire arrangement was traversed across the boundary layer at a lateral separation of 13 mm from the rake. This separation was the minimum possible, from the point of view of flow interference, with the present probe-support geometry. The effect of this separation on the comparison between different conditional techniques is discussed in §5. The X-wire/cold-wire arrangement was initially calibrated for velocity and yaw (the procedure indicated by Bradshaw (1971, pp. 123–124) was followed) and for temperature in the heated core of a plane jet. The X-wire (the hot-wire resistances were matched to within 1 %) was operated by two DISA 55M10 anemometers and DISA 55M25 linearizers. The contamination of the velocity signal by temperature was removed using a technique similar to that suggested by Champagne (1979). The contamination of the temperature signal by velocity was negligible (typically 0·006 °C/m s^{-1}), and no action was taken to remove it.

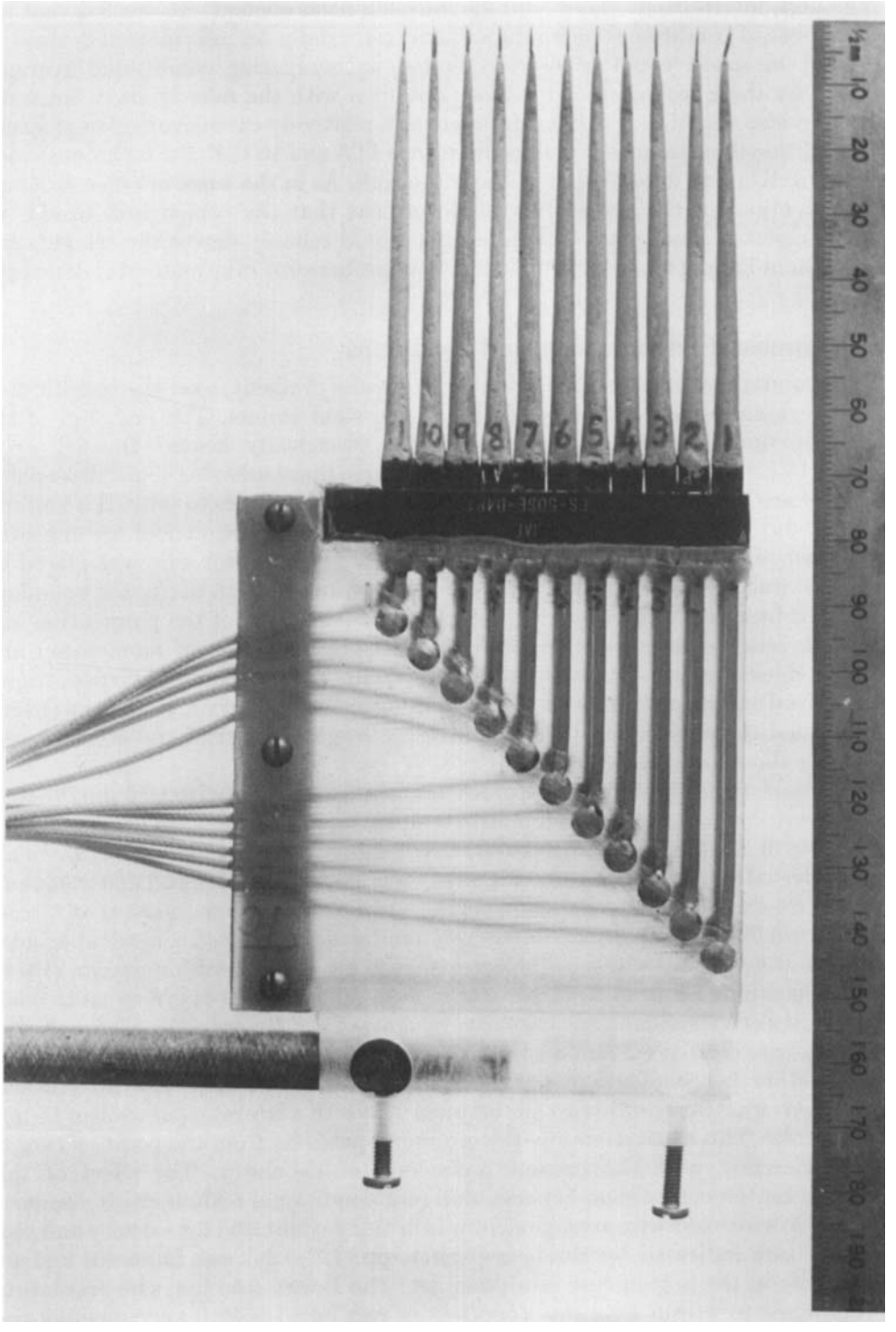

FIGURE 1. Cold-wire rake.

Signals from the rake and X-wire/cold-wire arrangement were recorded on an 8-channel FM tape recorder (HP3968A) at a speed of 38·1 cm s^{-1} and subsequently digitized at a sampling frequency of 8000 Hz. Prior to digitization, a low-pass Krohn–Hite filter (model 3343) with a cutoff frequency set at 4000 Hz was used. The duration of the digital records varied between 100 and 200 s. Signals proportional to u and v were obtained from the X-wire/cold-wire voltages using analogue computer elements with allowance for the temperature contamination of the velocity. Digital records were stored on tapes or discs and processed on a PDP 11/34 computer.

Measurements in this paper were made at a distance x from the trip of 2·24 m and a free-stream velocity U_1 of 8·4 m s^{-1}. At this station, the difference $T_w - T_1$ was 14 °C and the friction velocity U_τ and temperature T_τ were 0·33 m s^{-1} and 0·85 °C respectively. The displacement thickness δ_1 and momentum thickness δ_2 were 8·2 and 5·4 mm respectively. The Reynolds number R_m ($\equiv U_1\delta_2/\nu$) was 3100. The boundary-layer thickness δ, based on $U = 0{\cdot}99\ U_1$, was 47 mm, and the thermal-layer thickness, based on $T - T_1 = 0{\cdot}01\ (T_w - T_1)$, was 44 mm.

3. Conditional techniques definitions and description

In the conditional sampling and averaging techniques that are examined here, detection criteria are used to generate a conditioning function that attempts to lock the sampling onto a certain feature (in this case the occurrence of the temperature front) of the coherent structure. The conditioning function here consists of a series of time points $\tau_1, \tau_2, \ldots, \tau_n, \ldots, \tau_N$, where each point τ_n denotes the reference point (in time) when detection occurs, and N is the total number of structures. The output D of the detection algorithm is equal to unity at these particular values of τ_n and is zero for other values of the original digital time series. The conditional average of a function f is then given by

$$\langle f(t)\rangle = \frac{1}{N}\sum_{n=1}^{N} f(\tau_n + t).$$

Time $t = 0$ arbitrarily corresponds to the position where all the reference points τ_n are brought into alignment. In the present investigation, f stands for either u, v, θ or the products uv, $u\theta$, $v\theta$. Signals, u, v, θ are fluctuations relative to the conventional (long-time average) means so that $\bar{u} = \bar{v} = \bar{\theta} = 0$. In all conditional techniques described below, the detection and sampling occur at the same position in space, thus reducing the possibility of degradation of phase for the coherent structure that is captured. The variation in arrival time and trajectory of coherent structures, their inherent three-dimensionality and the strong likelihood that these structures arrive at the detecting probe at different ages or stages in their evolution are not considered here since the main concern is to compare the performance of different techniques which presumably detect a feature that is common to all these structures.

3.1. *VITA*

VITA (variable-interval time averaging) was used by Kaplan & Laufer (1968) to study the structure associated with the motion of the turbulent/non-turbulent interface in the outer part of a boundary layer. The variance of $\partial u/\partial t$, computed over a relatively short time interval, was large when the detecting probe (a single hot wire) was in the turbulent region and small when the wire was in the non-turbulent region of the flow. VITA has since been used, in only slightly modified form, by BK to detect bursts in the wall region ($y^+ < 100$) of the layer and by CB to detect the temperature

front throughout the whole layer. It should be made clear that while CB used a rake of cold wires to identify temperature fronts, their conditional averages were obtained with VITA. Here, D is set equal to 1 when the conditions

$$\tilde{\theta}^2 - \tilde{\theta}^2 > k\theta'^2, \tag{1a}$$

$$\dot{\tilde{\theta}} < 0 \tag{1b}$$

are first satisfied. The present identification of τ_n differs from that of CB, who used the midpoint of the pulse train generated by (1*a*, *b*) to identify τ_n. The prime denotes the conventional r.m.s. value of the whole signal, the dot denotes a time derivative, k is a threshold parameter and the tilde represents the moving average

$$\tilde{\theta} = \frac{1}{T}\int_{t-\frac{1}{2}T}^{t+\frac{1}{2}T} \theta(t)\,dt, \tag{2}$$

which is essentially a low-pass-filtering operation with cutoff at $\frac{1}{2}T$.

3.2. *HOLE*

The quadrant-analysis decomposition was used by Willmarth & Lu (1972) and Wallace, Eckelmann & Brodkey (1972) to sort out contributions to the (kinematic) Reynolds shear stress $\overline{uv}$ from the four quadrants of the (u, v)-plane. Grass (1971) has found that ejections ($u < 0$, $v > 0$) and sweeps ($u > 0$, $v < 0$) made nearly equal contributions to the turbulence production. Lu & Willmarth (1973) singled out ejections and sweeps that made particularly large contributions to $\overline{uv}$ by introducing a hyperbolic hole size. Strong ejections were identified when the magnitude of uv ($u < 0$, $v > 0$) exceeded the hole size or threshold $H = |uv|/u'v'$.

BK noted that the lack of phase information eliminated the possibility of defining a coherent structure from the u, v data. A similar comment was made by Van Atta (1980), who indicated that the geometry of the coherent structure could not be obtained from the quadrant-analysis decomposition. The use of a hole size does seem however to provide various options for generating the sequence of reference time points τ_n. D is set equal to 1 when

$$|uv| > Hu'v', \quad \text{and } |uv| \text{ is maximum,} \tag{3}$$

in the second quadrant ($u < 0$, $v > 0$) of the (u, v)-plane. Comte-Bellot, Sabot & Saleh (1979) obtained conditional averages of u, v and uv in a fully developed pipe flow using condition (3) to identify either ejections or sweeps. Averages were presented for several values of the threshold H.

3.3. *Brown–Thomas*

Brown & Thomas (1977) used a procedure (hereinafter referred to as BT)† in which the signal u is first low-pass filtered before forming a high-frequency component u_h by subtracting the filtered signal from the total signal. Thomas (1977), also Thomas & Brown (1977), used this procedure as part of a conditional technique to generate conditional averages of u, v, uv at various positions in a turbulent boundary layer. $D(t)$ is set equal to 1 when the rectified and smoothed high-frequency component of u exceeds a certain threshold level. In the present investigation, $D(t)$ is set equal to 1 when

$$\tilde{\theta}_h > k\tilde{\theta}'_h, \quad \text{and } \tilde{\theta}_h \text{ is maximum.} \tag{4}$$

† The procedure was also applied to a signal proportional to the wall shear stress in a turbulent boundary layer.

Unlike VITA and RA1 or RA3 (see below), this technique does not impose a condition on the sign of $\dot{u}$ or $\dot{\theta}$.

3.4. *RA1*

In this technique, used by Rajagopalan & Antonia (1981) in a turbulent mixing layer, the detection is based on the occurrence of large-amplitude peaks of $\dot{\theta}^3$. The use of $\dot{\theta}$ seems preferable to that of $\dot{u}$ (Rajagopalan & Antonia 1980) since it has been suggested that the non-zero value of the skewness of the temperature derivative in various shear flows reflects the anisotropy of the coherent large-scale motion (e.g. Sreenivasan, Antonia & Britz 1979). Although $\dot{\theta}^3$ has positive and negative peaks, negative peaks† have, on average, a larger amplitude than positive peaks, consistent with the negative skewness of $\dot{\theta}$. The detection function $D(t)$ is set equal to 1 when

$$\begin{gathered} \dot{\theta}^3 < k[(\dot{\theta})^3]', \\ \text{and} \quad (\dot{\theta})^3 \text{ is minimum.} \end{gathered} \tag{5}$$

3.5. *RA3*

This is an extension of the RA1 method in which use is made of all three signals (u, v and θ) instead of only θ in the detection method. Signals u, v, θ were first low-pass filtered (effective value of $T^+ = TU_\tau^2/\nu = 3{\cdot}7$) in order to focus the detection method on the relatively sudden changes in u and v associated with the internal shear layer (see e.g. CB). The identification by these latter authors of this shear layer with the temperature front provides some justification for the use of u, v and θ in the detection procedure. D is set equal to 1 when the six conditions

$$|\dot{\tilde{\alpha}}^3| > k(\dot{\tilde{\alpha}}^3)', \quad \dot{\tilde{u}} > 0, \quad \dot{\tilde{v}} < 0, \quad \dot{\tilde{\theta}} < 0 \tag{6}$$

are first satisfied. In (6), α stands for either u, v or θ.

3.6. *RAKE*

The conditional technique adopted in this paper as 'reference' for detecting the temperature front relies on the visual recognition of the front from simultaneous temperature traces obtained with the cold-wire rake. The temperature traces of figure 2, for $R_m = 3100$, reveal the slow increase in θ followed by a relatively sudden decrease. The front is observed at earlier times as the distance increases from the wall, the inclination of the front to the wall being caused by the mean shear in the flow (Subramanian & Antonia, (1979) found that the convection speed of the front was approximately equal to the local mean velocity). As found by CB, the front is not always detected by all sensors of the rake, an observation that reflects the inherent three-dimensionality of the structure, the randomness of its spatial trajectory or the age of the structure at the instant of detection. The possibility that these three effects occur in combination cannot be easily rejected. For pragmatic reasons, formal recognition of a front by inspection of computer plotted traces of θ occurred whenever the front was identified over a sufficiently large range of y/δ, in the present case $0{\cdot}1 < y/\delta < 0{\cdot}7$. A temperature front is shown in figure 2 marked by arrows. Although about 80 % of the fronts detected could be observed over the range $0{\cdot}04 < y/\delta < 0{\cdot}97$, there were occasions when the front was not detectable at the probe locations nearest the wall or the edge of the layer. For example, it is difficult to identify the front clearly in the lowest trace ($y^+ = 15$) of figure 2.

To compensate for the possibility of slightly different arrival times of the front at the y-location of the X-wire/cold-wire arrangement and at the same y-location of the

† Positive peaks are dominant in the mixing layer of a slightly heated jet since the skewness is of opposite sign to that in the boundary layer.

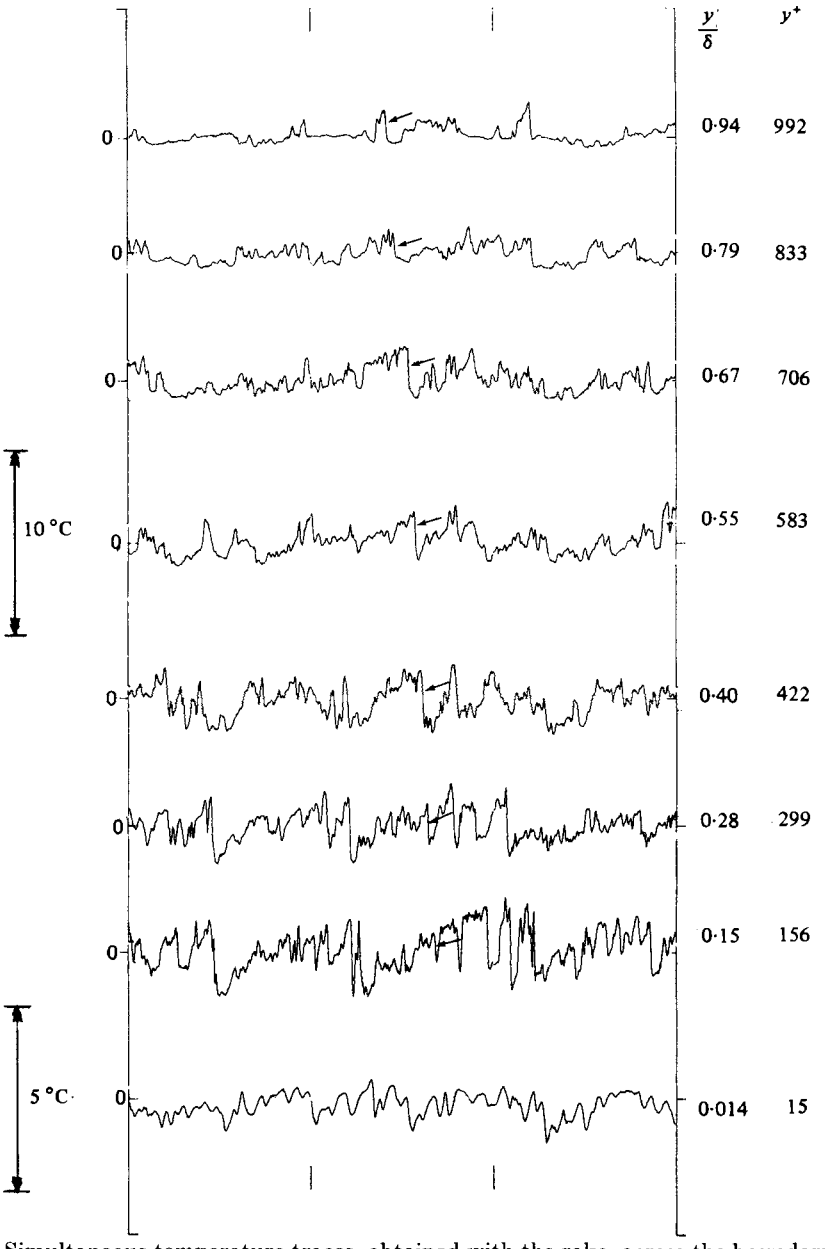

FIGURE 2. Simultaneous temperature traces, obtained with the rake, across the boundary layer at $R_m = 3100$. Time increases from left to right. The vertical scale of 10 °C applies to all traces except for $y^+ = 15$. Horizontal time span = $17{\cdot}3\,\delta/U_1$. Arrows denote one particular temperature front.

rake, the arrival times used in RAKE were those corresponding to the arrival of the front at the X-wire/cold-wire. Whenever a temperature front was detected with the rake the temperature signal from the cold wire of the X-wire/cold-wire arrangement was examined. It was found that this signal always exhibited a sharp decrease in temperature when the front was observed on the rake. Although differences between the occurrence of this temperature decrease and the location of the front were sometimes observed, these differences were of either sign and small (much smaller than differences in arrival time at neighbouring wire positions in the rake) and the

Method	Threshold k			$U_1\bar{t}_1/\delta$			Correspondence between fronts		
	$y/\delta = 0{\cdot}04$	0·32	0·75	0·04	0·32	0·75	0·04	0·32	0·75
RAKE	—	—	—	2·63	2·63	2·63	100	100	100
VITA	0·6	0·7	0·55	2·43	2·81	2·55	42	43	51
HOLE	1·9	2·1	2·5	2·78	2·60	2·58	15	11	20
BT	2·7	2·6	2·6	2·86	2·66	2·67	32	36	31
RA1	3·2	3·0	1·7	2·64	2·67	2·59	42	38	51
RA3	0·2	0·2	0·2	2·50	2·50	5·0	30	24	37

TABLE 1. Correspondence between fronts detected by rake and other conditional techniques

cold wire in the X-wire/cold-wire arrangement could in fact be considered as a member of the rake for the purpose of detecting the large-scale front. The values of τ_n, at a particular y, are obtained by applying RA1, with a small value of k, to the temperature signal from the cold wire in the X-wire/cold-wire arrangement. The number of fronts used in forming the RAKE average is provided by the rake of cold wires and not by RA1.

4. Selection of detection parameters

Most of the conditional techniques described in the previous section rely on setting a discrimination or threshold level and a hold time. Previous investigators have examined in detail the effect of k and T on the resulting conditional averages and, in particular, on the frequency of detection. Ideally, this frequency and both the shape and amplitude of the conditional averages should remain independent of k and T, at least over some appropriately selected range for these parameters. This ideal result is not achieved in practice and, for a given value of T, the number of detections shows a monotonic decrease as k increases. There does not appear to be an objective way of choosing k and T, the final choice of k and T being usually made after visual comparison of locations where $D \equiv 1$ with the original signal or signals used in the detection method. To evaluate the performance of the various conditional techniques, it was decided to choose k and T so that the number of detections per unit time yielded by each technique was approximately equal to the detection frequency estimated by visual examination (RAKE) of simultaneous temperature traces similar to those in figure 2. This approach is similar to that adopted by Offen & Kline (1973), who selected their detection parameters by forcing agreement of detection frequency with the flow-visualization frequency. Values of k used at three values of y/δ are given in table 1. The same value of T^+, equal to 3·7, is used in VITA, BT and RA3. A hold time is not used in HOLE and RA1. Also indicated in the table are values of $\bar{t}_1$, the average duration between fronts. The value of $U_1\bar{t}_1/\delta = 2{\cdot}63$ estimated with RAKE is not very different from the value of about 3·0 estimated by CB using VITA. It should be noted that this technique does not, for a particular selection of k and T, provide a unique value of $\bar{t}_1$ across the boundary layer. The frequency ($\equiv \bar{t}_1^{-1}$) of detection reported in CB decreases for $y/\delta < 0{\cdot}1$.

It seems appropriate to comment on and compare the values of k and T given in the table with those selected in previously reported investigations using these techniques. The values of k and T^+ used for VITA are significantly smaller than those used by CB and BK. These latter authors used $k = 1{\cdot}2$ and $T^+ = 10$, while CB adopted $k = 0{\cdot}9$ and $T^+ = 11{\cdot}7$. EK found that their conditional averages did not depend

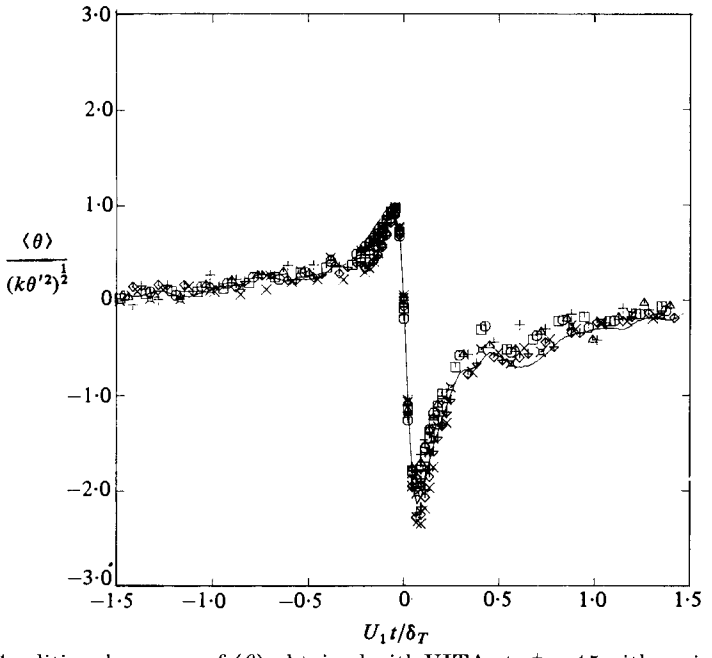

FIGURE 3. Conditional average of $\langle\theta\rangle$ obtained with VITA at $y^+ = 15$ with various threshold levels. $T^+ = 3{\cdot}7$. ×, $k = 0{\cdot}6$; ◇, 0·8; ▽, 1·0; ——, 1·2; ⊓, 1·4; □, 1·6; ○, 1·8; △, 2·0; +, 2·5.

strongly on T^+. In the present work, $U_1\bar{t}_1/\delta$ was found to remain approximately constant, at a particular value of k, when T^+ was varied between 8 and 12. For a value of T^+ in this range, the detection frequency f decreased appreciably as k was increased. BK found that although the amplitude of $\langle u\rangle/u'$ varied by a factor of about two when k was increased from 0·9 to 2·5, distributions of $\langle u\rangle$ normalized by $k^{\frac{1}{2}}u'$ seemed to fall onto a single curve. This observation was interpreted as indicating the deterministic value of the eddy structure whose velocity signature had been educed. When the present distributions of $\langle\theta\rangle$ at $y^+ = 15$ (figure 3) are normalized by $k^{\frac{1}{2}}\theta'$ the result is similar to that shown in figure 16 of BK. For the range of k used in figure 2, the maximum change in $\langle\theta\rangle$ near $t = 0$ was found to increase by about 70 % as k increased from 0·6 to 2·5. The change in the magnitude of $\langle\theta\rangle/k^{\frac{1}{2}}\theta'$ near $t = 0$ in figure 3 is considerably sharper than the corresponding change in $\langle u\rangle/k^{\frac{1}{2}}u'$ obtained in BK. Also, whereas the results of BK suggest a systematic increase in the maximum change in $\langle u\rangle$ as k is increased, such a trend is not apparent in figure 3. These differences can probably be attributed to the inclusion of the sign of $\tilde{\theta}$ in the detection criterion used in figure 3; no discrimination was made in BK between rapid decelerations and rapid accelerations. It will be shown later that rapid decelerations are associated with a relatively sharp increase in temperature, but their frequency of occurrence is small enough for the qualitative features of the conditional average of $\langle\theta\rangle$ to remain unaffected when the condition $\tilde{\theta} < 0$ is removed from the conditions given by (1).

For HOLE, the threshold $H(\equiv k)$ was set equal to about 2·0 to obtain the same value of $\bar{t}_1$ as yielded by RAKE. This value of H is significantly smaller than the value of about 4·5 (or $|uv| \geqslant 10|\overline{uv}|$) used by Lu & Willmarth (1973) to identify violent ejections. For this value of H, these authors found that contributions from the sweep quadrant to $\overline{uv}$ are negligible and that the mean period $\bar{t}_e$ between violent ejections remains approximately constant across the boundary layer. Their normalized period

$U_1\bar{t}_e/\delta$ is about 4·3, which corresponds to a frequency approximately 60 % smaller than the present frequency of temperature fronts. Both $\bar{t}_e$ and the mean period $\bar{t}_s$ between sweeps increase rapidly as H increases. For $H \approx 2$, Lu & Willmarth's results indicate that $U_1\bar{t}_e/\delta \approx 1{\cdot}7$ and $U_1\bar{t}_s/\delta \approx 3{\cdot}7$.

The present value of k of 2·7 used with BT is almost twice as large as that ($k = 1{\cdot}5$) chosen by Thomas & Brown. However, these latter investigators selected a value of T^+ significantly larger than the present value of 3·7; they used a filter cutoff of $2\pi\delta_1/TU_1 = 0{\cdot}43$ to generate the smoothed rectified high-frequency detection signal. For the low ($R_m = 4920$) and high ($R_m = 10200$) Reynolds numbers investigated by Thomas (1977), this filter cutoff setting corresponds to values of T^+ of about 131 and 122 respectively. Beljaars (1979) reports conditional averages of u in a boundary layer at $R_m = 1550$ based on a detection procedure in which the u-signal (at $y^+ = 15$) is first high-pass filtered then squared and smoothed before comparison with a threshold level. This detection procedure, not unlike BT, bears close similarity to VITA. Beljaars notes that serious problems arose in the selection of the threshold and filter frequency, since significant variations in detection frequency were observed for only small changes in the detection parameters. However, Beljaars, Thomas, BK and Rajagopalan & Antonia (1981), have all indicated that the qualitative behaviour of the conditional averages, though not their amplitude, is not sensitive to the selection of the detection parameters. In the present investigation, it was found that, for BT, an increase in k from 2 to 3 resulted in a 35 % increase in the maximum change in $\langle\theta\rangle$ near $t = 0$. For RA1, which does not require a hold time, the corresponding increase was 42 % when k was increased from 1 to 5 (times the r.m.s. value of $\hat{\theta}^3$).

5. Results and discussion

In figures 4 and 5† are compared conditional averages of u, v, θ obtained by the different techniques at $y/\delta = 0{\cdot}04$ ($y^+ = 40$) and 0·32 respectively. Figure 6 shows a comparison of conditional averages of the products uv, $u\theta$ and $v\theta$ at $y/\delta = 0{\cdot}32$. The normalization used to present the information on conditional averages in these and other figures is that generally adopted by other investigators; conditional averages of u, v and θ are normalized by the respective conventional r.m.s. values of these signals. Conditional averages of uv, $u\theta$ and $v\theta$ are normalized by the (kinematic) Reynolds shear stress $\overline{uv}$, and (thermometric) heat fluxes $\overline{u\theta}$ and $\overline{v\theta}$ respectively.

While there is qualitative agreement between all but one of the techniques (HOLE is the conspicuous exception), quantitative agreement can only be regarded as poor. In particular, differences in the magnitude and location of the relatively sudden changes in the conditional averages are evident near $t = 0$. VITA, BT and RA3 detect the front at approximately the same time, but this time occurs later than that at which the front is detected by RA1 (and RAKE). This discrepancy can be associated with the use of a hold time in one-point techniques, with the exception of RA1. For RA1, $t = 0$ corresponds to the position where $\hat{\theta}^3$ reaches a local minimum after falling below the appropriate threshold level. The good agreement between RAKE and RA1 with regard to the location $t = 0$ is artificial since, as mentioned earlier, RA1, with a small value of the threshold k, is used to identify the location $t = 0$ for RAKE. Any other one-point technique, with a small value of k, could have been used to generate

† With the exception of figures 1 and 11, all figures have been plotted by the Zeta plotter (model 1453) attached to the 11/34 computer. Each point in the digital time series was plotted and no smoothing was applied.

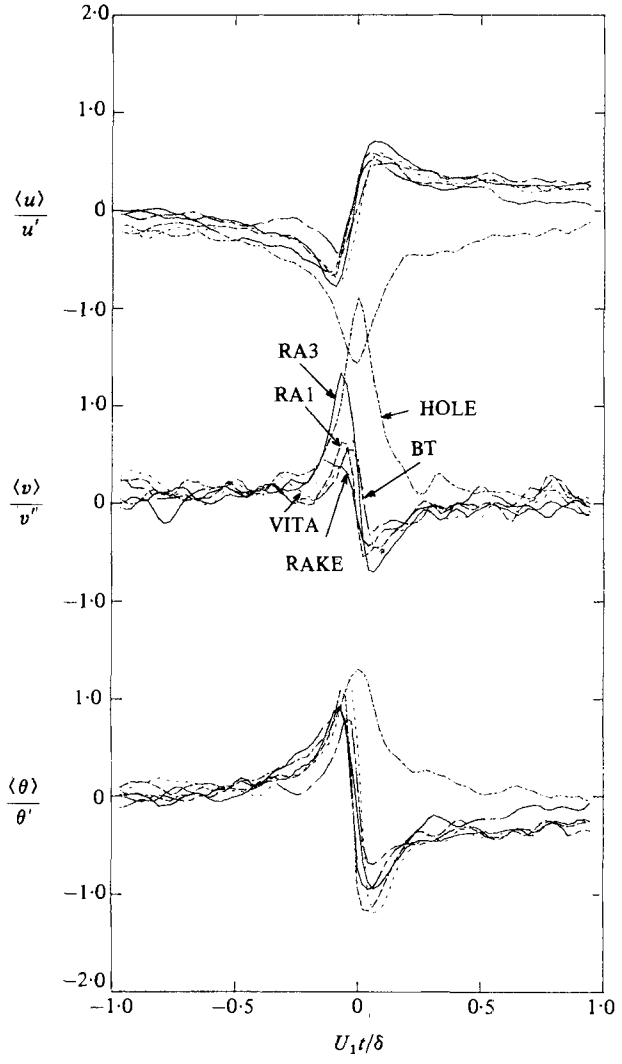

FIGURE 4. Comparison of conditional averages of u, v, θ obtained by different conditional techniques at $y^+ = 40$. $N = 100$. ——·——, RAKE; ·····, VITA; – – –, HOLE; — — — —, BT; ——, RA3; – – – –, RA1.

the values of τ_n for RAKE, with the obvious consequence that there would be no time shift between the RAKE average and that generated by that one-point technique. While the actual location of the RAKE averages in figures 4, 5, 6 is immaterial, the shape and amplitude of the averages do not depend on which particular technique is used to generate τ_n for RAKE. The differences between RAKE and other techniques in figures 4, 5, 6 are genuine and not affected by the spanwise separation between the rake and the X-wire/cold-wire. For HOLE, condition (3) is applied when (u, v) is in the second quadrant; this may explain why a change in the signs of $\langle u \rangle$, $\langle v \rangle$ and $\langle \theta \rangle$ is not detected near $t = 0$. The maximum values of $\langle v \rangle$, $\langle \theta \rangle$ and the minimum value of $\langle u \rangle$ occur at $t = 0$. These values like those for the products, are significantly larger than the corresponding maxima or minima obtained by other techniques. The maximum change in $\langle v \rangle$ near $t = 0$ as obtained by RA3 is also significantly larger than that provided by other techniques. This large change in $\langle v \rangle$,

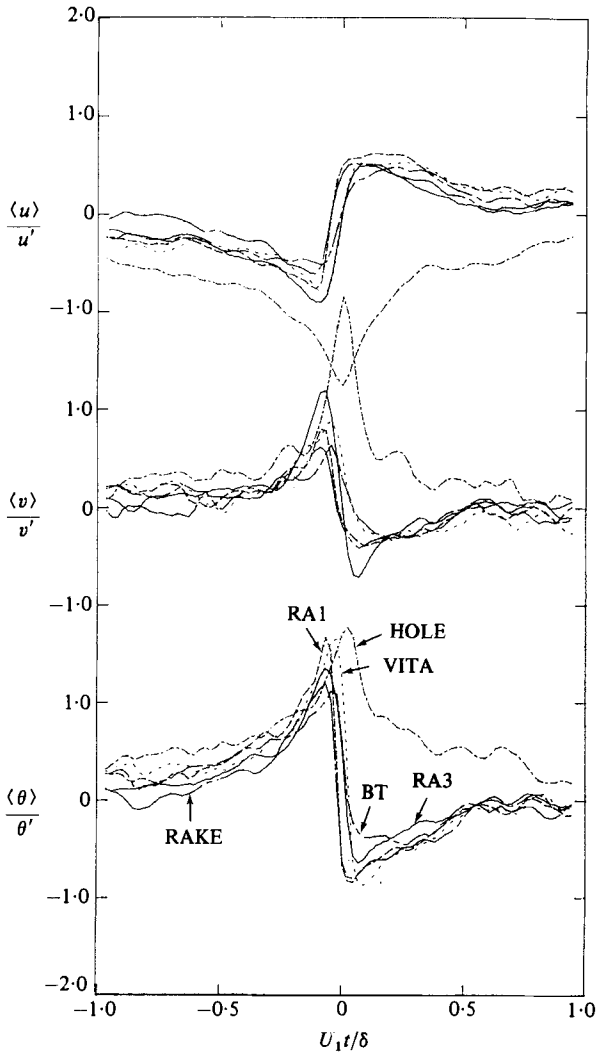

FIGURE 5. Comparison of conditional averages of u, v, θ obtained by different conditional techniques at $y/\delta = 0{\cdot}32$. $N = 100$. Symbols are as for figure 4.

apparently due to the specific inclusion of v in (6), is reflected in the relatively large changes, near $t = 0$, in $\langle uv \rangle$ (figure 6*a*) and $\langle v\theta \rangle$ (figure 6*c*).

Conditional averages presented in figures 4–6 were obtained for a total of 100 fronts. The effect of the record duration (or, more appropriately, the number of fronts detected) on the conditional averages obtained by several techniques was examined in detail. Only the results for VITA are shown here (figures 7 and 8) since they represent fairly closely those obtained for other techniques. The effect of N is slightly larger for $\langle v \rangle$ than for either $\langle u \rangle$ or $\langle \theta \rangle$. The effect of N on $\langle u \rangle$ or $\langle \theta \rangle$ is not significant. Oscillations exhibited by $\langle v \rangle$ (figure 7) for $N = 100$ and 200 disappear for $N = 400$ and 800. In the case of products (figure 8), the conditional average $\langle u\theta \rangle$ appears to be less affected by the magnitude of N than $\langle uv \rangle$ or $\langle v\theta \rangle$. This is not too surprising since the correlation coefficient $-\overline{u\theta}/u'\theta'$ is larger (across the boundary layer) than $-\overline{uv}/u'v'$ or $\overline{v\theta}/v'\theta'$. Since $N = 100$ is adequate for computing stable conditional averages of $\langle u \rangle$, $\langle v \rangle$, $\langle \theta \rangle$, the differences in $\langle u \rangle$, $\langle v \rangle$, $\langle \theta \rangle$ in figures 4 and 5 can only

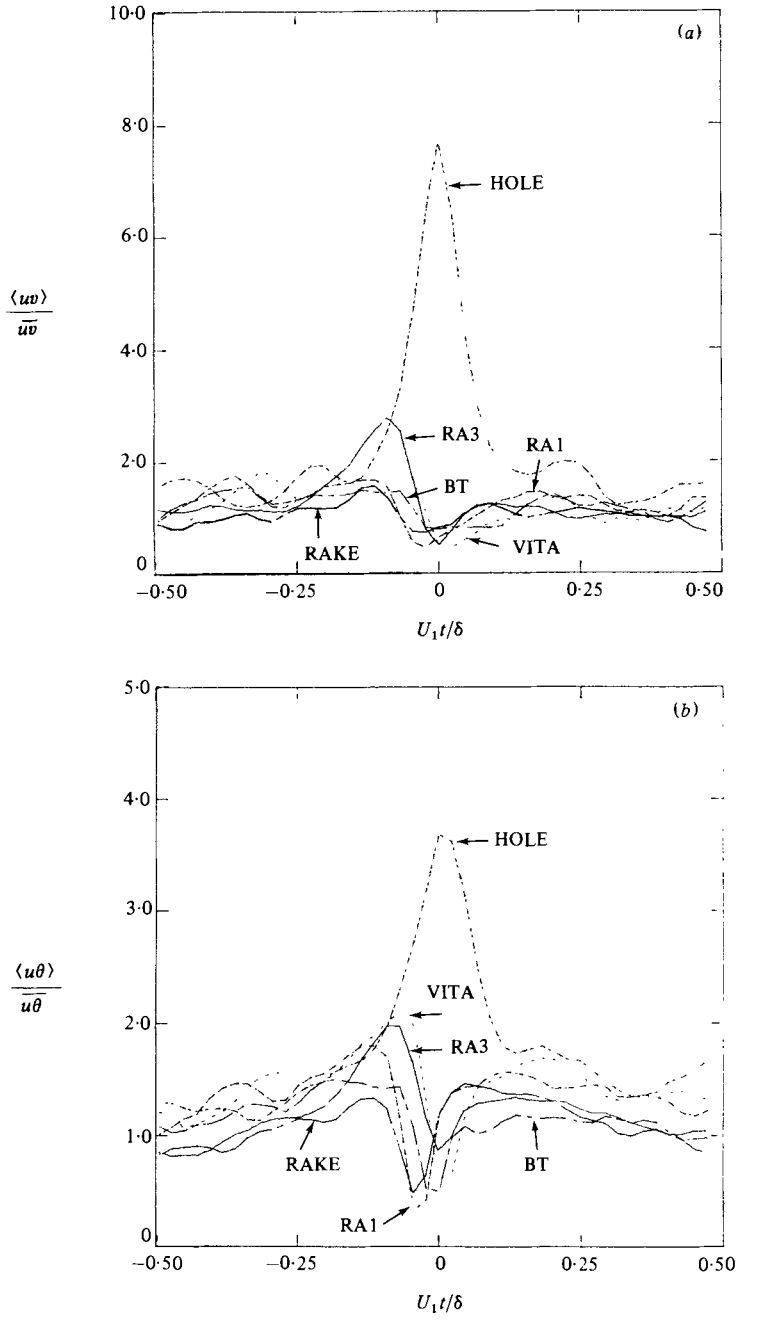

FIGURE 6. For caption see facing page.

be considered to be genuine and cannot be attributed to an insufficient record duration. In the case of $\langle v\theta \rangle$ and, especially, $\langle uv \rangle$ the effect of N is evident for both positive and negative values of t, sufficiently removed from the region associated with the relatively large changes in $\langle \theta \rangle$ and also $\langle u \rangle$ and $\langle v \rangle$. For example, the peaks noticed on $\langle uv \rangle$ and $\langle v\theta \rangle$, for $N = 100$ and 200, at $U_1 t/\delta \approx -0{\cdot}4$, are not apparent when $N = 400$ or 800. These results, together with those for $\langle v \rangle$ in figure 6, suggest that N should have been chosen equal to about 400 to ensure convergence of

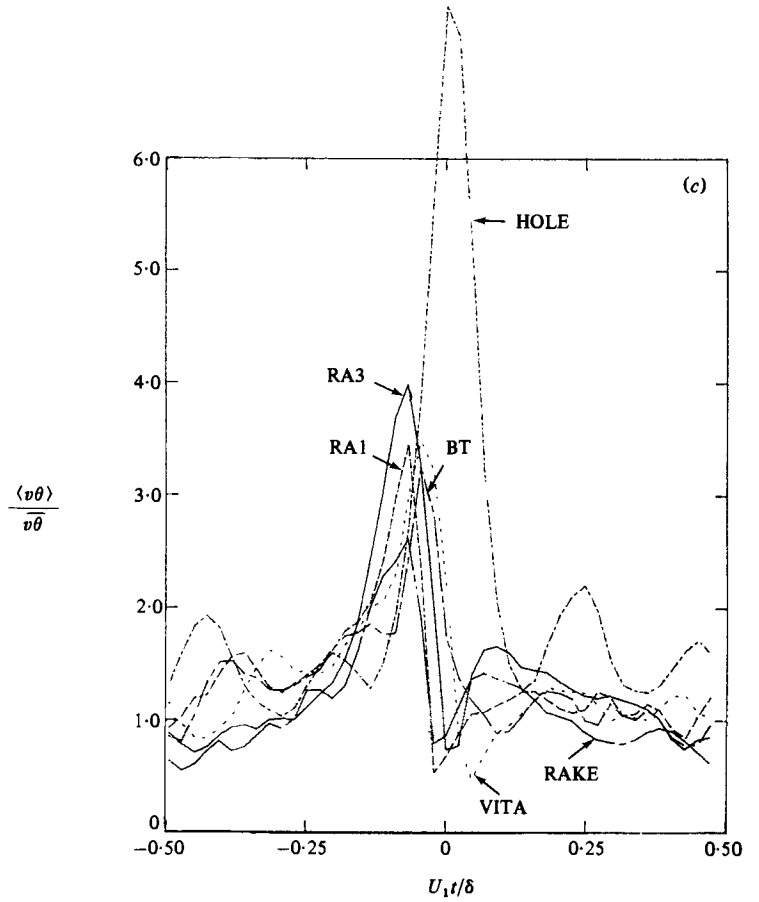

FIGURE 6. Comparison of conditional averages of products uv, $u\theta$ and $v\theta$ obtained by different conditional techniques at $y/\delta = 0{\cdot}32$. $N = 100$. (*a*) $\langle uv \rangle / \overline{uv}$; (*b*) $\langle u\theta \rangle / \overline{u\theta}$; (*c*) $\langle v\theta \rangle / \overline{v\theta}$. Symbols are as for figure 4.

conditional averages of $\langle v \rangle$ and of the products $\langle uv \rangle$ and $\langle v\theta \rangle$. However, it was decided that the extra work involved in identifying 400 (instead of 100) fronts in RAKE was not essential as it would not affect conditional averages in the region of interest, i.e. the region immediately prior to and following the identification of the front. It should be emphasized however that local oscillations observed in figure 6 at relatively large values of $U_1|t|/\delta$ are probably spurious.

A further qualification with regard to interpreting conditionally averaged products seems to be in order. Degradation of these averages is expected to increase rapidly as time $|t|$ increases from the instant of detection of the front in view of the three-dimensionality of the structures and their different stages of evolution at detection. Such degradation, more important for products than individual fluctuations, would make the interpretation of conditionally averaged products difficult.

While differences exist in the magnitude of the change in conditional averages near $t = 0$, there is reasonable agreement between VITA and RA1 with respect to either the individual signals or the products. Figure 6 indicates that the maximum change and slope near $t = 0$ of conditional averages of products obtained by RAKE are smaller than those provided by other techniques. This result reflects the fact that the fronts detected by RAKE, although coherent in space, are not necessarily all

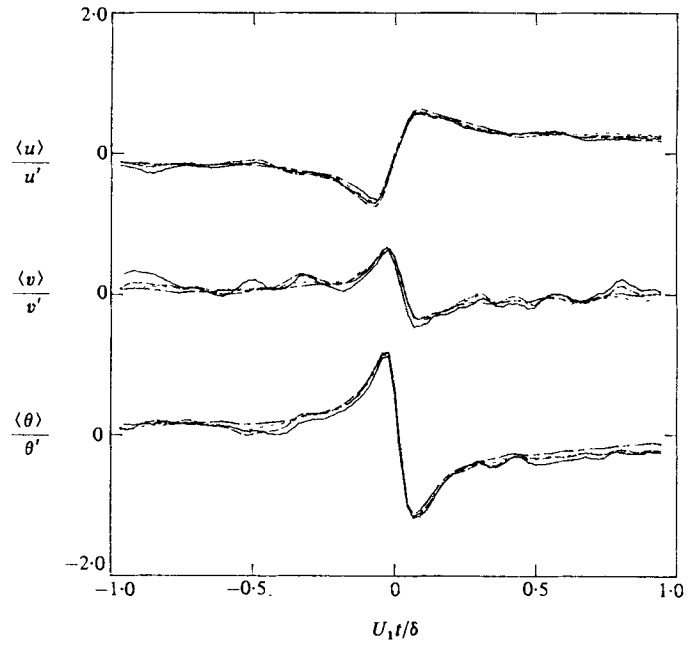

FIGURE 7. Effect of sample size on conditional averages obtained at $y^+ = 40$ with VITA – individual signals. ——, $N = 100$; – – –, 200; - - - - -, 400; – – –, 800.

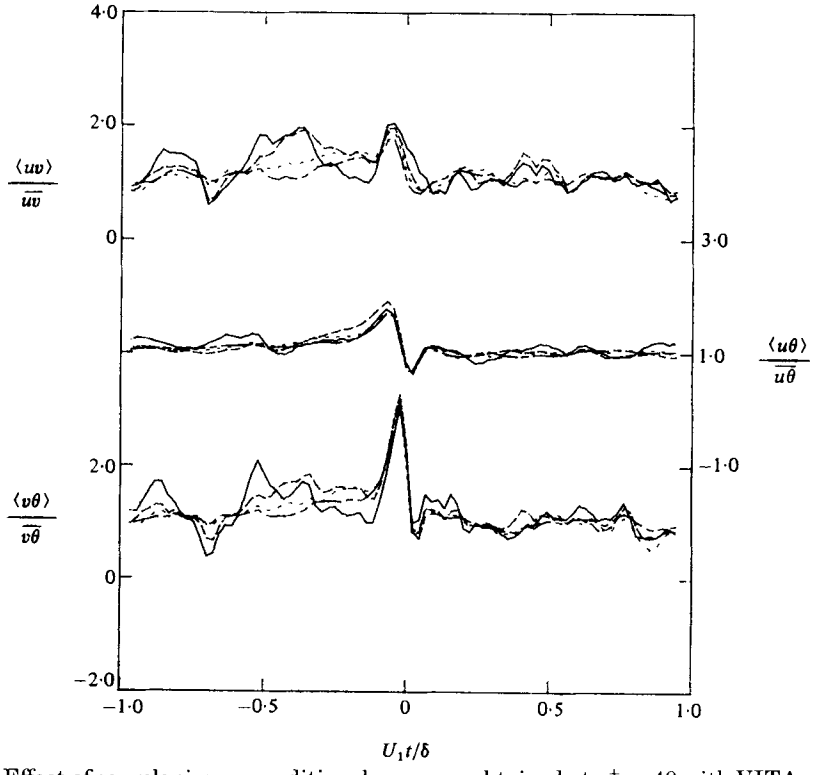

FIGURE 8. Effect of sample size on conditional averages obtained at $y^+ = 40$ with VITA – products. Symbols are as for figure 7.

sharp; VITA and RA1, as a consequence of the conditions imposed in (1) and (5), focus on relatively sharp changes in θ, which are not necessarily always associated with a coherent front. That this is the case is evident in table 1, which shows that, out of the 100 fronts detected by RAKE, approximately 42 are found by VITA and RA1 at $y/\delta = 0{\cdot}04$. The correspondence decreases for BT and RA3, and only 15 fronts are detected by HOLE. When the RAKE method is applied to the 42 events that are common to RAKE, VITA and RA1, the resulting conditional averages (figure 9) exhibit larger amplitudes and gradients near $t = 0$ when compared with the results obtained for the total number (100) of fronts detected in the record. When RAKE is applied to only the 7 fronts detected by all techniques, a further increase is observed in the amplitude and gradient (in the case of products) near $t = 0$. The relatively large oscillations observed for both positive and negative values of time when $N = 7$ are without doubt due to the very small number of samples used to form the conditional averages.

The spanwise separation Δz between the rake and the X-wire/cold-wire arrangement is approximately 280 viscous units ($\Delta z^+ \approx 280$) at $R_m = 3100$. Since the average spanwise wavelength of the longitudinal sublayer streaks is about 100 viscous units, information about bursting is precluded from the present comparison between one-point techniques and RAKE.

CB found that as the wall was appoached (y/δ less than about 0·10) the zero-crossings of $\langle u \rangle$ and $\langle v \rangle$ occurred at earlier times than the zero-crossings of $\langle \theta \rangle$. The X-probe/cold-wire configuration used by CB was similar to that in the present study, so that the phase shift between $\langle \theta \rangle$ (measured at a location upstream of the X-probe) and $\langle u \rangle$ or $\langle v \rangle$ is in a direction opposite to that determined in the experiment. CB accepted their result as genuine and indicated that a possible interpretation is that the temperature front and shear layer are not coincident. It was also suggested that the phase shift may be caused by the spanwise velocity component associated with streamwise vortices in the wall region of the flow. A time delay was applied to the digital time series for θ to correct† for the longitudinal separation between the X-probe and the cold wire. For the present Reynolds number, the delay, normalized by U_τ^2 and ν, was equal to 1·8.

Present distributions of $\langle u \rangle$, $\langle v \rangle$, $\langle \theta \rangle$ at $y^+ = 40$ (figure 4) cross the time axis at approximately the same location. At this Reynolds number, measurements with the X-probe at smaller values of y^+ were not possible. However measurements at $y^+ = 15$, made at $R_m \approx 990$, did not indicate a phase shift between $\langle u \rangle$ or $\langle v \rangle$ and $\langle \theta \rangle$. This provides some support for the coincidence of the 'internal shear layer' and temperature front in a region of the flow immediately outside the linear sublayer, at least for low Reynolds numbers.

When the signals u and v are used, instead of θ, in the detection procedure of VITA, the resulting conditional averages (figure 10) appear to reflect the choice of the signal used for detection. Values of k and T^+ were changed (for u, $k = 0{\cdot}4$, $T^+ = 9{\cdot}2$; for v, $k = 0{\cdot}9$, $T^+ = 5{\cdot}5$) to ensure that $U_1 \bar{t}_1/\delta$ remained approximately equal to the value obtained by using θ. It is clear in figure 10(*a*) that the use of a particular signal in the detection criterion results in enhancement of the conditional average of that particular signal near $t = 0$. Both the amplitude and the gradient of the conditional average are increased near $t = 0$. The effect is more significant for $\langle v \rangle$ than for either $\langle u \rangle$ or $\langle \theta \rangle$. Conditional averages obtained with RAKE are included in figure 10 for comparison. The use of v in the detection method leads to maximum values of $\langle uv \rangle / \overline{uv}$ and $\langle v\theta \rangle / \overline{v\theta}$ that are significantly larger than those corresponding to the use of u

† All conditional averages in the present paper have been corrected for this delay.

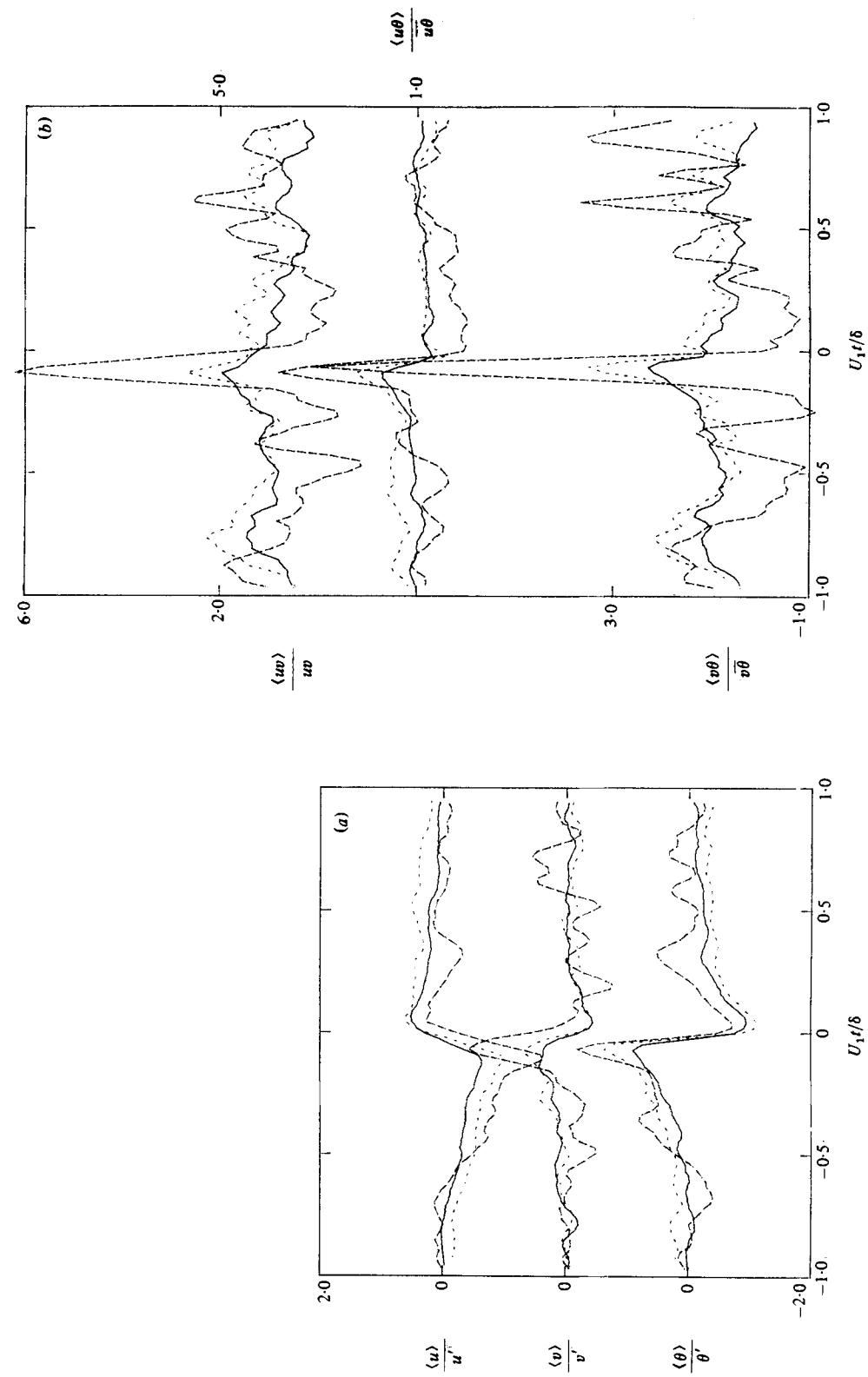

FIGURE 9. Comparison of conditional averages using RAKE for different numbers of detected fronts. $y^+ = 40$. ——, $N = 100$ (all fronts detected are included in average); - - - -, $N = 42$ (fronts included are those common to RAKE, VITA, RA1); — —, $N = 7$ (fronts common to all techniques). (*a*) Individual signals; (*b*) products.

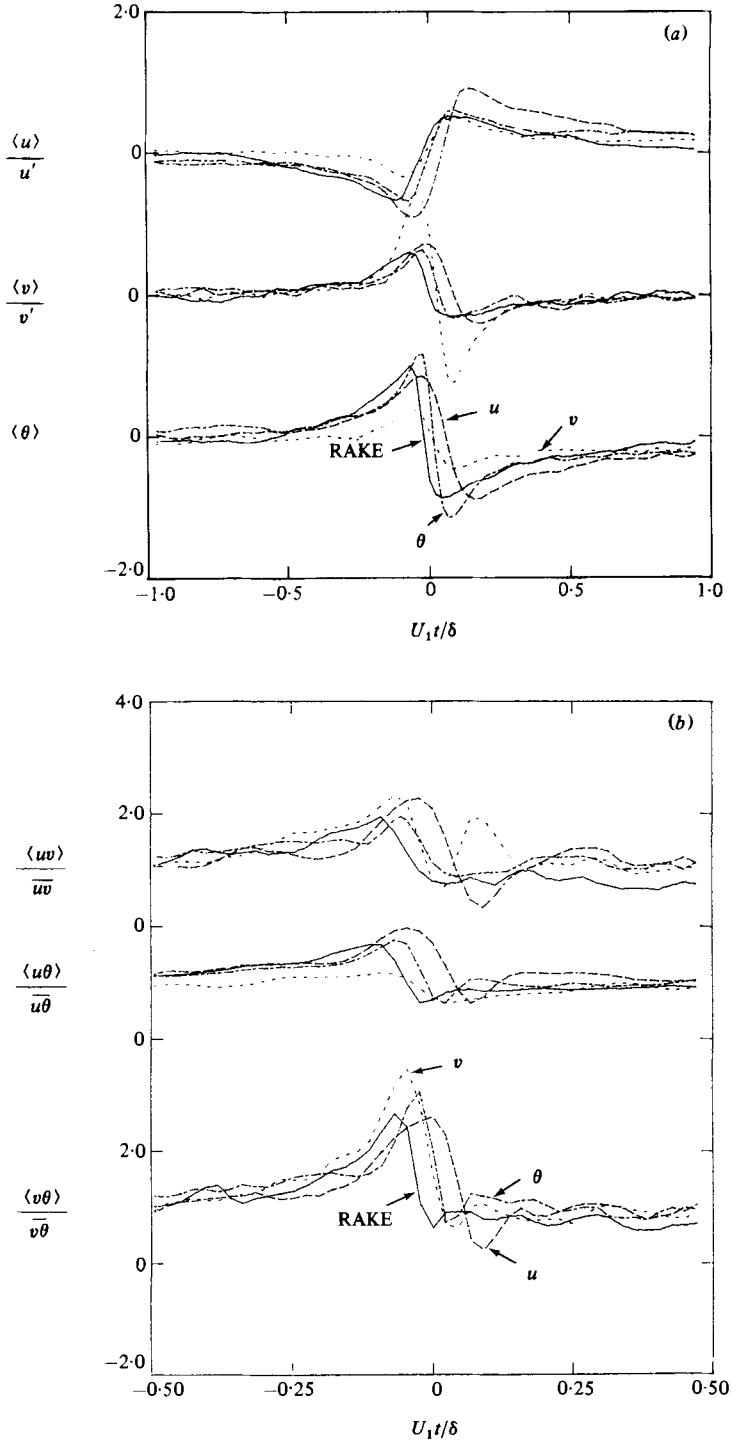

FIGURE 10. Conditional averages obtained at $y^+ = 40$ by VITA when the detection criterion is based on different signals. $N = 400$ for VITA; $N = 335$ for RAKE. ——, Based on u; – – –, θ; · · · ·, v; ——, RAKE. (*a*) Individual signals; (*b*) products.

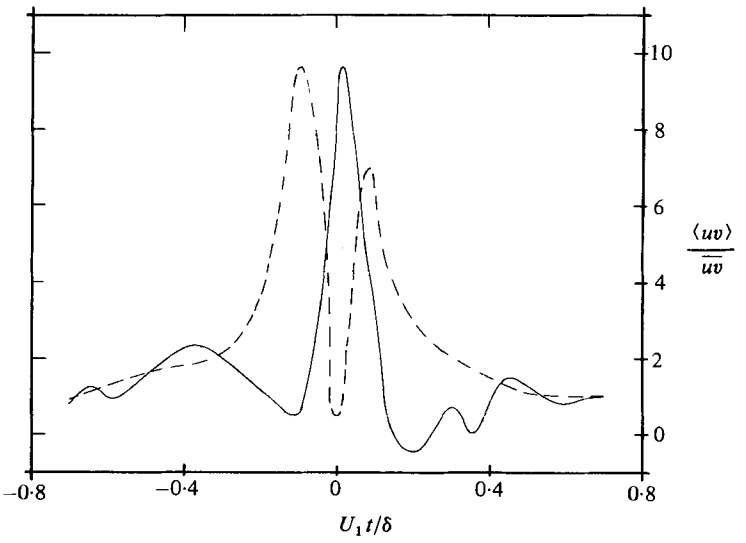

FIGURE 11. Conditional averages of product uv obtained outside the sublayer. ——, BK, $R_m = 2550$; $y^+ = 15$; ——, Chen (1975), 2820, 18.

or θ in the detection. In this context, it is of interest to note (figure 11) that the conditional average of uv presented by BK is significantly different from that obtained by Chen (1975) at a comparable value of y^+ and R_m. Although VITA was used for both sets of results, BK used u in the detection procedure (no condition was imposed on $\dot{u}$), whereas θ was used by Chen. It seems difficult, however, to attribute the difference between the two conditional averages in figure 11 to the effect observed in figure 10(b), since the use of u instead of θ does not really lead to an enhancement of $\langle uv \rangle$ near $t = 0$. Instead, a completely different signature, characterized by two peaks on either side of $t = 0$, was obtained by BK (figure 11). It should also be noted that the $\langle v \rangle$ signature reported by Chen (1975) at $y^+ \approx 18$ is quite different from that found in BK (at $y^+ = 15$).

CB found, prior to adding the condition $\dot{\theta} < 0$ to (1), that not all temperature fronts detected by VITA consisted of rapid coolings: about 20 % of the detections consisted of warm 'fronts'. From observations of the rake traces, CB assumed that the warm fronts were due to the random background and not to any coherent structure. For the present data, with $k = 0{\cdot}7$ and $T^+ = 3{\cdot}7$, about 25 % of detections at $y/\delta = 0{\cdot}32$ consisted of warm fronts. Conditional averages for u and v were computed for the number of fronts corresponding to the temperature rises. The number of warm fronts was approximately equal to the number (100) of cold fronts, so that the record duration for warm-front averages was approximately four times longer than that used for rapid coolings. The results (figure 12a) indicate that associated with the rise in $\langle \theta \rangle$ near $t = 0$ is an increase in $\langle v \rangle$ and a corresponding decrease in $\langle u \rangle$. The magnitudes of the gradients in these quantities are comparable to those related to the rapid coolings. Maximum values of the normalized products (figure 12b) occur for positive values of t in the case of warm fronts; for rapid coolings, these maxima were obtained prior to the instant of detection. The observation that the warm fronts are occasionally registered† by several sensors of the rake and the evidence of figure 12

† These fronts, like the rapid coolings, are also inclined to the surface and are first detected by sensors further away from the wall. The coherence of warm fronts in the outer part of the layer ($0{\cdot}54 < y/\delta < 1{\cdot}15$) can in fact be observed in figure 4 of CB. This coherence has also been observed in present θ-traces over a wider range of y/δ.

are not conclusive but seem to point to the possibility that the warm front may demarcate the boundary of a sweep that is usually followed by an ejection. In contrast, the more frequent rapid cooling may be identified with the boundary of an ejection that is usually followed by a sweep. The double-peaked behaviour of $\langle uv \rangle$, which is strongly evident (figure 11) in the results of BK at $y^+ = 15$, is less prominent in the present results. Small positive peaks occur in all the conditional products at small positive values of t in figures 6 and 12 (*b*). Such behaviour would seem to support the speculation that a sweep usually follows an ejection in this region of the layer. The relative magnitude of the $\langle uv \rangle$ peaks on either side of $t = 0$ appears to be in qualitative agreement with the contributions to the Reynolds shear stress from the second and fourth quadrants of a (u, v)-plane quadrant analysis at corresponding values of y/δ. Wallace *et al* (1977) obtained conditional averages of uv based on the detection of a characteristic pattern of u (a relatively weak deceleration followed by a strong acceleration) in a fully developed turbulent duct flow with a relatively thick viscous sublayer. These averages indicate a single contribution from the sweep within the sublayer. At $y^+ \approx 10$, twin maxima are noticeable, and at $y^+ \approx 15$, the contribution from the ejection becomes larger than that due to the sweep. Eckelmann & Wallace (1980) emphasized the similarities between the pattern recognition technique and VITA, but also noted significant differences. In particular, the maximum $\langle uv \rangle$ found by the pattern-recognition search is almost one order of magnitude smaller than that obtained with VITA at $y^+ = 15$.

It is of interest to compare conditional averages obtained, over a relatively wide range of y/δ, by different conditional techniques. Conditional averages, presented in figures 13 and 14, were obtained by VITA and RA3. For VITA, T^+ was kept constant at 3·7, and k was varied to maintain a constant value, independent of y/δ, for the average duration between detections. For RA3, neither k nor T^+ were changed, and the average duration $\bar{t}_1$, constant for $y/\delta < 0{\cdot}5$, increased in the outer part of the layer (at $y/\delta = 0{\cdot}64$ and 0·9, $U_1\bar{t}_1/\delta$ was about 4 and 8 respectively). Figures 13 and 14 indicate obvious qualitative agreement between the two techniques. Averages $\langle u \rangle$, $\langle v \rangle$ and $\langle \theta \rangle$ change markedly in shape as y/δ increases. Distributions of $\langle \theta \rangle$, $\langle u \rangle$, $\langle v \rangle$ are approximately antisymmetrical with respect to $t = 0$ at $y/\delta = 0{\cdot}04$ and become skewed (positively for $\langle \theta \rangle$ and $\langle v \rangle$, negatively for $\langle u \rangle$) as y/δ increases. At $y/\delta = 0{\cdot}9$ all three averages exhibit a plateau at positive values of $U_1\bar{t}_1/\delta$.

Quantitative agreement between VITA and RA3 is not good: maximum values obtained with RA3 are larger than those computed with VITA. This is especially evident in the case of $\langle v \rangle$ and the products $\langle uv \rangle$ (figure 14) and $\langle v\theta \rangle$ (not shown here). The difference between the peak values of $\langle uv \rangle$ and $\langle v\theta \rangle$, as yielded by the two techniques, is close to two. Note that the mild double peak appearance of $\langle uv \rangle$, evident at $y/\delta = 0{\cdot}04$ and 0·32, disappears at the larger values of y/δ. This result is obtained for both techniques and is also observed for $\langle u\theta \rangle$ and $\langle v\theta \rangle$.

6. Concluding discussion

The primary result that emerges from this experimental investigation is the relatively poor correlation that exists between the detection of the front found by several conditional techniques and that estimated by visual observation of simultaneous temperature signals from a rake of temperature sensors. This latter estimate, while containing some degree of subjectivity, is based on information obtained over a straight line in space and seems preferable to conditional techniques based on information at only one point in the flow. The best correspondence with detections by RAKE was found for VITA and RA1. The best correspondence was only 51 %

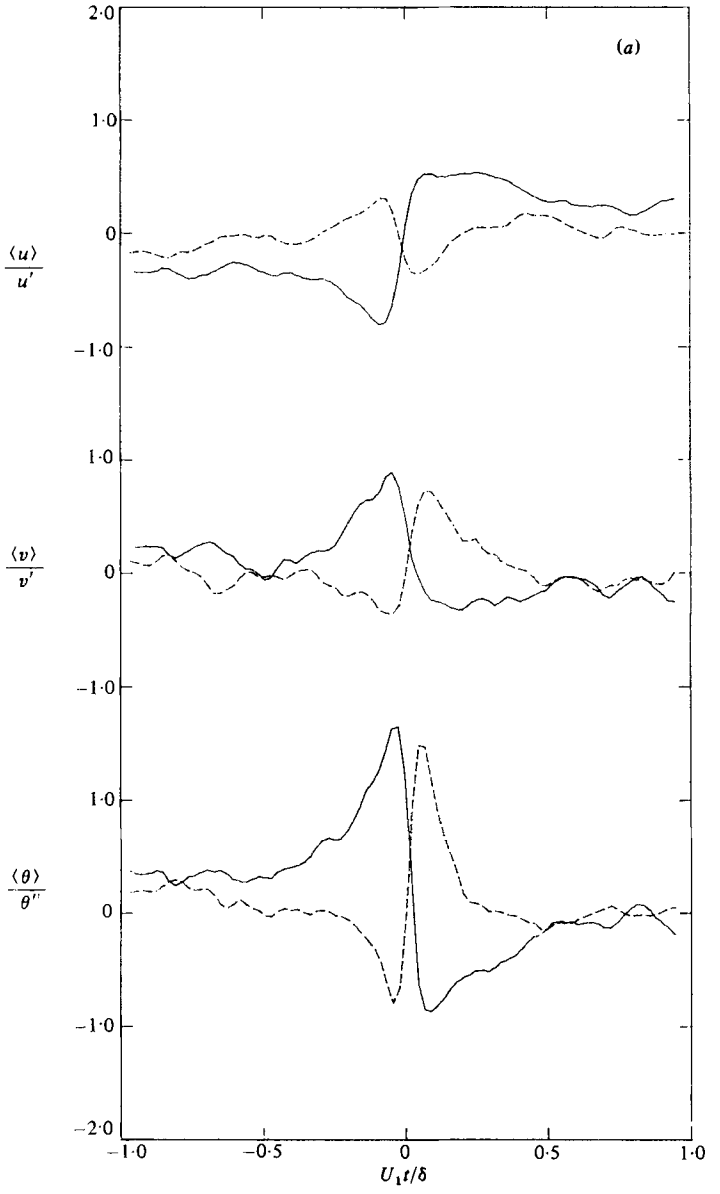

FIGURE 12. For caption see facing page.

and did not seem to depend on the particular value of y at which the conditional techniques were applied. The conditional technique (BT) of Thomas & Brown (1977) and RA3, a technique developed in the course of the present work, achieved a correspondence of about 30 %. The smallest correspondence was obtained for HOLE, which focused essentially on fronts characterized by large excursions in velocity, temperature and their products. Despite the relatively poor correspondence between the conditional techniques, these techniques, with the exception of HOLE, produce conditional averages that exhibit all the qualitative features found by RAKE. It is evident that a significant percentage of fronts detected by RAKE are not associated with large excursions in velocities u, v or in the product uv. Quantitatively, the

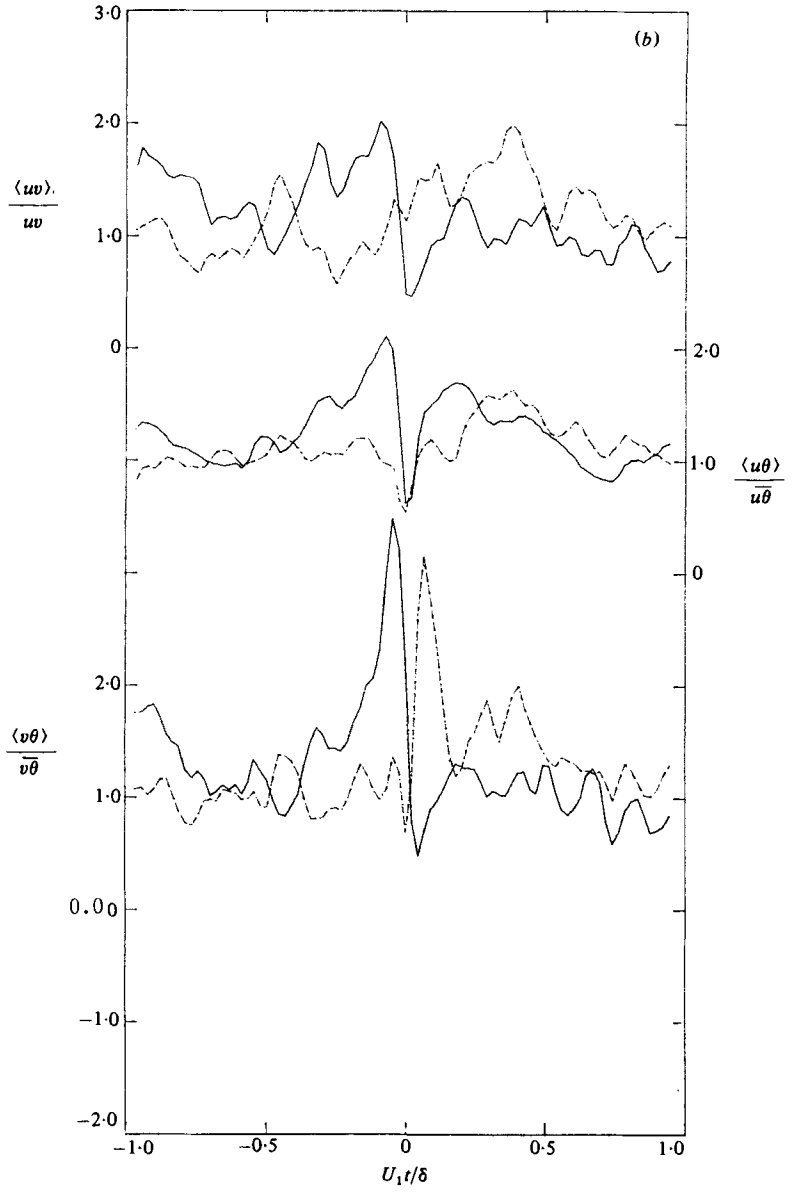

FIGURE 12. Conditional averages obtained at $y/\delta = 0{\cdot}32$ by VITA with the detection criterion based on θ and different signs of $\dot{\theta}$. ——, $\dot{\theta} < 0$ ($N = 100$); – – – –, $\dot{\theta} > 0$ ($N = 97$). (*a*) Individual signals; (*b*) products.

maximum amplitude and gradient of conditional averages near $t = 0$ is generally larger for the one-point conditional techniques than for RAKE. It does appear, however, that this latter method, although perhaps cumbersome to implement, offers one important advantage over the one-point techniques, which tend to focus on features of the motion associated with large excursions of uv or $v\theta$ but not necessarily associated with the coherent large-scale motion in the layer. For this reason, RAKE should be preferred to one-point techniques when estimating contributions of the large-scale motion of the layer to the Reynolds shear stress and heat flux. With the exception of HOLE, one-point techniques should, however, continue to play a useful

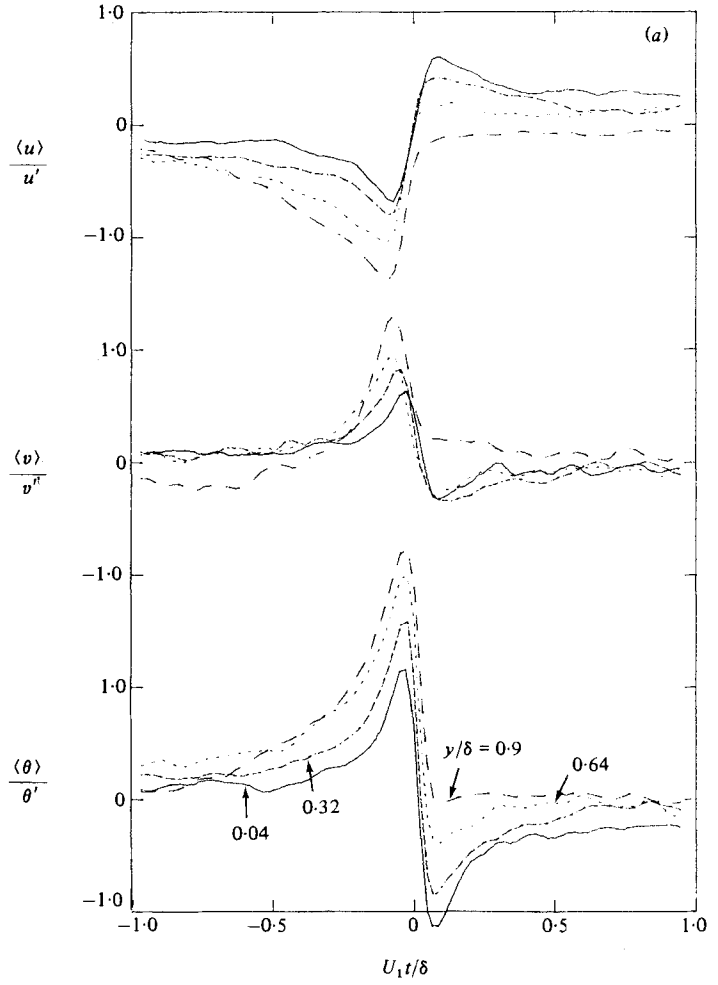

FIGURE 13. For caption see facing page.

role in determining, at least qualitatively, the effect of parameters such as pressure gradient, Reynolds number and surface conditions on the large scale motion.†

The primary result of this investigation bears similarity to the finding of Offen & Kline (1973) that none of the one-point detection schemes they investigated correlated well with the flow-visualization indications of bursting, although most of these schemes were as effective as the visual data at detecting periods of large uv. It should be emphasized, however, that the present comparison of different techniques cannot be expected to include information on bursting in view of the lateral separation between the rake and X-wire/cold-wire arrangement. Also excluded from the present comparison is information about typical eddies (Falco 1977) whose spanwise length scale is of order 200 viscous units. The present use of RAKE is, however, such that RAKE averages are not degraded by the lateral separation, and the comparison between RAKE and one-point techniques is not invalidated.

In contrast with the rapid coolings associated with the fronts detected by RAKE,

† Antonia *et al.* (1982) used VITA to determine the influence of Reynolds number on the ensemble averages associated with the temperature front.

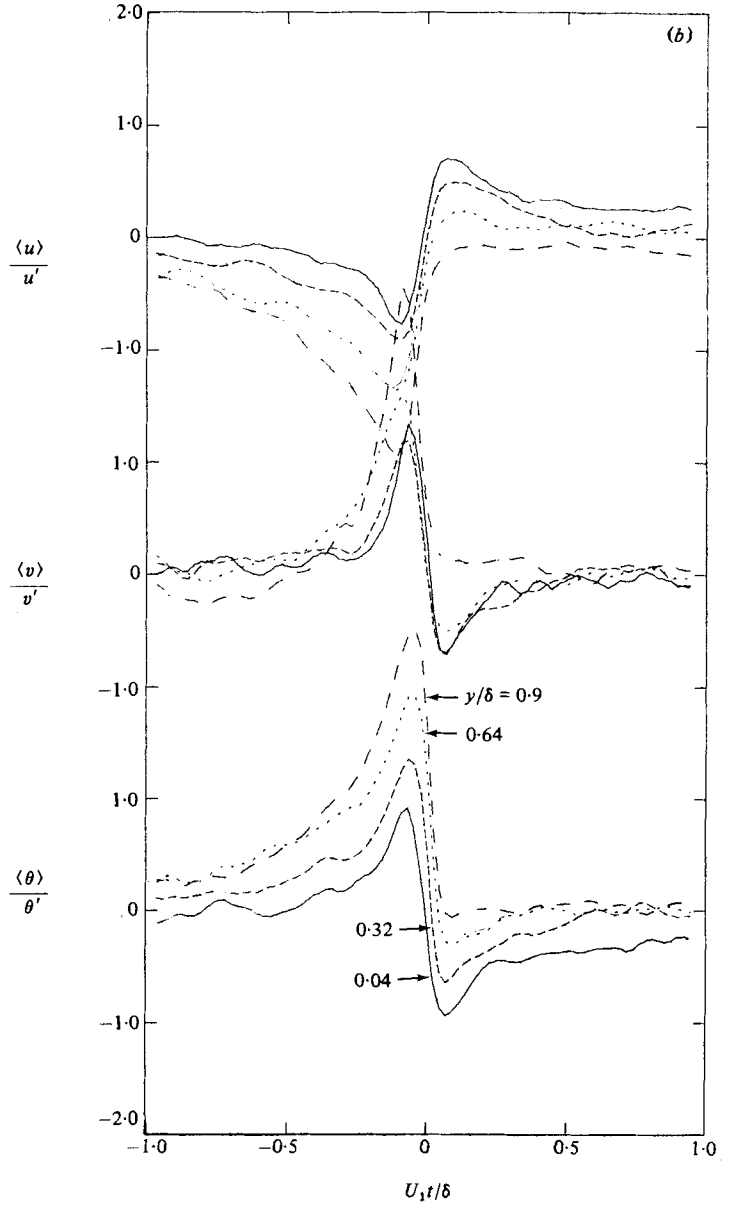

FIGURE 13. Comparison of conditional averages across the boundary layer obtained using VITA and RA3. ——, $y/\delta = 0{\cdot}04$; – – –, 0·32; · · · · ·, 0·64; – – –, 0·90. (*a*) VITA ($N = 400$); (*b*) RA3 ($N = 150$).

relatively sharp temperature rises are occasionally detected by the one-point conditional techniques when no constraint on the sign of the temperature gradient is imposed. The possibility that these temperature jumps are strictly associated with the random turbulent motion and not with any coherent motion is not supported by the present experimental evidence. Conditional averages indicate that the sharp rise in $\langle\theta\rangle$ is accompanied by a decrease in $\langle u\rangle$ and a concomitant increase in $\langle v\rangle$. Peak values of $\langle uv\rangle$, $\langle u\theta\rangle$ and $\langle v\theta\rangle$ occur at times later than the instant of detection. This result and the observation that warm fronts are occasionally registered by several sensors of the rake support the speculation that the warm front may demarcate the

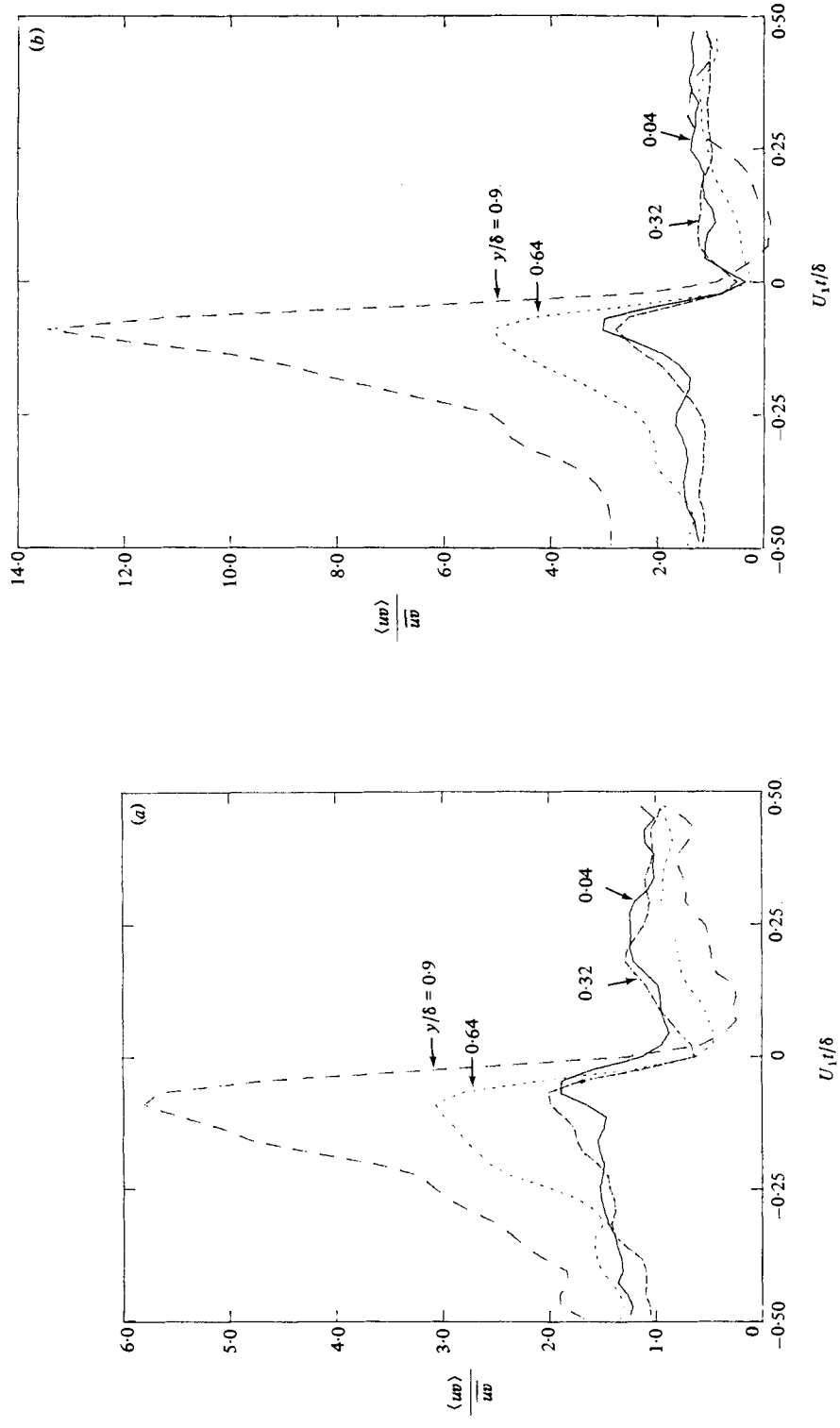

FIGURE 14. Comparison of conditional averages of product uv across the boundary layer obtained using VITA and RA3. (*a*) VITA ($N = 400$); (*b*) RA3 ($N = 150$). Symbols are as for figure 13.

boundary of a sweep that is usually followed by an ejection. Speculatively, the more commonly occurring rapid cooling would demarcate a boundary of an ejection that is usually followed by a sweep. The present conditional averages of uv and those obtained by other investigators seem to underline the importance of contributions by ejections and sweeps to the Reynolds shear stress.

The support of the Australian Research Grants scheme is gratefully acknowledged. The help of Messrs R. Scobie, M. Ooms, I. Miller and the workshop staff with the design and construction of the rake is also appreciated.

REFERENCES

ANTONIA, R. A. 1980 The organized motion in a turbulent boundary layer. In *Proc. 7th Australasian Conf. on Hydraulics and Fluid Mechanics, Brisbane*, pp. 155–162.

ANTONIA, R. A. 1981 Conditional sampling in turbulence measurement. *Ann. Rev. Fluid Mech.* **13**, 131–156.

ANTONIA, R. A., RAJAGOPALAN, S., SUBRAMANIAN, C. S. & CHAMBERS, A. J. 1982 Reynolds-number dependence of the structure of a turbulent boundary layer. *J. Fluid Mech.* **121**, 123–140.

BELJAARS, A. 1979 A model for turbulent exchange in boundary layers. Ph.D. thesis, Eindhoven University of Technology, Holland.

BLACKWELDER, R. F. & KAPLAN, R. E. 1976 On the wall structure of the turbulent boundary layer. *J. Fluid Mech.* **76**, 89–112.

BRADSHAW, P. 1971 *An Introduction to Turbulence and Its Measurement*. Pergamon.

BROWN, G. L. & THOMAS, A. S. W. 1977 Large structure in a turbulent boundary layer. *Phys. Fluids Suppl.* **20**, S243–S252.

CHAMPAGNE, F. G. 1979 The temperature sensitivity of hot wire. In *Proc. Dynamic Flow Conf. – Dynamic Measurements in Unsteady Flows, 1978, Marseille/Baltimore*, pp. 101–114.

CHEN, C. H. P. 1975 The large scale motion in a turbulent boundary layer: a study using temperature contamination. Ph.D. thesis, University of Southern California.

CHEN, C. H. P. & BLACKWELDER, R. F. 1978 Large-scale motion in a turbulent boundary layer: a study using temperature contamination. *J. Fluid Mech.* **89**, 1–31.

COMTE-BELLOT, G., SABOT, J. & SALEH, I. 1979 Detection of intermittent events maintaining Reynolds stress. In *Proc. Dynamic Flow Conf. – Dynamic Measurements in Unsteady Flows, 1978, Marseille/Baltimore*, pp. 213–229.

CORINO, E. R. & BRODKEY, R. S. 1969 A visual investigation of the wall region in turbulent flow. *J. Fluid Mech.* **37**, 1–30.

ECKELMANN, G. & WALLACE, J. M. 1980 A comparison of characteristic features of coherent turbulent structures found using the variable interval time average (VITA) technique and using the pattern recognition technique. In *The Role of Coherent Structures in Modelling Turbulence and Mixing* (ed. J. Jimenez). Lecture Notes in Physics, vol. 136, pp. 292–303. Springer.

FALCO, R. E. 1977 Coherent motions in the outer region of turbulent boundary layers. *Phys. Fluids Suppl.* **20**, S124–S132.

GRASS, A. J. 1971 Structural features of turbulent flow over smooth and rough boundaries. *J. Fluid Mech.* **50**, 233–256.

HEAD, M. R. & BANDYOPADHYAY, P. 1978 Combined flow visualization and hot-wire measurements in turbulent boundary layers. In *Proc. Workshop on Coherent Structures of Turbulent Boundary Layers, Lehigh University*, pp. 98–129.

HEAD, M. R. & BANDYOPADHYAY, P. 1981 New aspects of turbulent boundary-layer structure. *J. Fluid Mech.* **107**, 297–338.

KAPLAN, R. E. 1973 Conditional sampling techniques. In *Turbulence in Liquids* (ed. G. K. Patterson & J. L. Zakin), pp. 274–283. University of Missouri–Rolla.

KAPLAN, R. E. & LAUFER, J. 1968 The intermittently turbulent region of the boundary layer. *University of Southern California Rep.* USCAE110.

KLINE, S. J., REYNOLDS, W. C., SCHRAUB, F. A. & RUNSTADLER, P. W. 1967 The structure of turbulent boundary layers. *J. Fluid Mech.* **30**, 741–774.

LU, S. S. & WILLMARTH, W. W. 1973 Measurements of the structure of the Reynolds stress in a turbulent boundary layer. *J. Fluid Mech.* **60**, 481–512.

OFFEN, G. R. & KLINE, S. J. 1973 Experiments on the velocity characteristics of 'bursts' and on the interactions between the inner and outer regions of a turbulent boundary layer. *Stanford University Dep. Mech. Engng Rep.* MD-31.

OFFEN, G. R. & KLINE, S. J. 1975 A comparison and analysis of detection methods for the measurement of production in a boundary layer. In *Turbulence in Liquids* (ed. G. K. Patterson & J. L. Zakin), pp. 289–318. University of Missouri–Rolla.

PERRY, A. E. & HOFFMANN, P. H. 1976 An experimental study of turbulent convective heat transfer from a flat plate. *J. Fluid Mech.* **77**, 355–368.

RAJAGOPALAN, S. & ANTONIA, R. A. 1980 Interaction between large and small scale motions in a two-dimensional turbulent duct flow. *Phys. Fluids* **23**, 1101–1110.

RAJAGOPALAN, S. & ANTONIA, R. A. 1981 Properties of the large structure in a slightly heated turbulent mixing layer of a plane jet. *J. Fluid Mech.* **105**, 261–281.

SREENIVASAN, K. R., ANTONIA, R. A. & BRITZ, D. 1979 Local isotropy and large structures in a heated turbulent jet. *J. Fluid Mech.* **94**, 745–775.

SUBRAMANIAN, C. S. 1981 Some properties of the large scale structure in a slightly heated turbulent boundary layer. Ph.D. thesis, University of Newcastle, Australia.

SUBRAMANIAN, C. S. & ANTONIA, R. A. 1979 Some properties of the large structure in a slightly heated turbulent boundary layer. In *Proc. 2nd Int. Symp. on Turbulent Shear Flows, London*, pp. 4.18–4.21.

SUNYACH, M. 1971 Contribution à l'étude des frontières d'écoulements turbulents libres. Thèse Docteur d'Etat, Université de Lyon, France.

THOMAS, A. S. W. 1977 Organized structures in turbulent boundary layers. Ph.D. thesis, University of Adelaide, Australia.

THOMAS, A. S. W. & BROWN, G. L. 1977 Large structure in a turbulent boundary layer. In *Proc. 6th Australasian Conf. on Hydraulics and Fluid Mechanics, Adelaide*, pp. 407–410.

VAN ATTA, C. W. 1980 Conditional sampling techniques. In *Handbook of Turbulence*, vol. 2. Plenum.

WALLACE, J. M., BRODKEY, R. S. & ECKELMANN, H. 1977 Pattern recognized structures in bounded turbulent shear flows. *J. Fluid Mech.* **83**, 673–693.

WALLACE, J. M., ECKELMANN, H. & BRODKEY, R. S. 1972 The wall region in turbulent shear flow. *J. Fluid Mech.* **54**, 39–48.

WILLMARTH, W. W. & LU, S. S. 1972 Structure of the Reynolds stress near the wall. *J. Fluid Mech.* **55**, 65–92.